

Providing Oligonucleotides with Steric Selectivity by Brush-Polymer-Assisted Compaction

Xueguang Lu,[†] Thanh-Huyen Tran,[‡] Fei Jia,[†] Xuyu Tan,[†] Sage Davis,[†] Swathi Krishnan,[‡] Mansoor M. Amiji,[‡] and Ke Zhang^{*,†}

[†]Department of Chemistry and Chemical Biology and [‡]Department of Pharmaceutical Sciences, School of Pharmacy, Bouvé College of Health Sciences, Northeastern University, Boston, Massachusetts 02115, United States

S Supporting Information

ABSTRACT: Difficult biopharmaceutical characteristics of oligonucleotides, such as poor enzymatic stability, rapid clearance by reticuloendothelial organs, immunostimulation, and coagulopathies, limit their application as therapeutics. Many of these side effects are initiated via sequence-specific or nonsequence-specific interactions with proteins. Herein, we report a novel form of brush-polymer/DNA conjugate that provides the DNA with nanoscale steric selectivity: Hybridization kinetics with complementary DNA remains nearly unaffected, but interactions with proteins are significantly retarded. The relative lengths of the brush side chain and the DNA strand are found to play a critical role in the degree of selectivity. Being able to evade protein adhesion also improves in vivo biodistribution, thus making these molecular nanostructures promising materials for oligonucleotide-based therapies.

Nucleic acids (NAs) and derivatives have been envisioned as biopharmaceutical agents in many forms of therapies, including oncolytic virotherapy,¹ suicide gene therapy,² anti-angiogenesis,³ therapeutic vaccines,⁴ and RNA interference/antisense gene-silencing therapies.⁵ However, unlike antibodies, NAs are not directly part of the natural biological defense system. Utilizing them as therapeutics faces an uphill battle against stability and delivery issues,⁶ and many sequence- and/or chemical-structure-specific nonhybridization activities such as stimulation of the immune system and coagulopathies.⁷

For oligonucleotides, although nuclease stability can be improved by chemical modification of the phosphodiester backbone, e.g., phosphorothioates,⁸ LNAs,⁹ PNAs,¹⁰ morpholinos,¹¹ ribose 2'-O-alkyl modifications,¹² and others, problems such as immune system stimulation and delivery to target site still plague development. Cationic materials, e.g., polymers, peptides, nanoparticles, liposomes, and others, have been designed to form polyplexes with NAs to assist cell entry, endosomal release, and codelivery of a drug.¹³ However, these materials remain largely limited to in vitro applications because their benefits in vivo are oftentimes overshadowed by carrier-induced side effects.¹⁴ Therefore, a system that can improve nuclease stability, preserve target-binding capability, minimize off-target effects, and improve biodistribution, e.g., passive tumor targeting, may prove to be the important missing link in achieving broad application of oligonucleotide-based therapies.

Recently, a class of NA nanostructure consisting of densely arranged oligonucleotides (spherical nucleic acids, SNA) has emerged.¹⁵ Despite the sterics created by the high-density arrangement, SNAs remain hybridizable with complementary strands.¹⁶ Furthermore, SNAs show increased stability against enzymatic degradation and can enter cells and regulate cellular gene expression without using a polycationic carrier.¹⁷

Inspired by the structure of the SNA, we have designed and synthesized a novel form of brush-polymer/DNA conjugate, termed pacDNA (polymer-assisted compaction of DNA). We hypothesize that the compaction of DNA by high-density side chains of brush polymers can provide the DNA with selective accessibility, favoring a complementary DNA strand to species with larger cross-section dimensions such as proteins (Scheme 1). The majority of unwanted, nonhybridization side effects are preceded by protein recognition of the oligonucleotide, be it degradation, toll-like receptor activation, or interferon response, and inhibition of the coagulation cascade.⁷ In principle, the steric selectivity resulting from the densely compacted structure of pacDNA can circumvent many of the side effects associated with protein binding. Given that the mechanism of DNA shielding is by steric hindrance (as opposed to electrostatic polyplexation), polymer compositions not typically considered for DNA protection can now be utilized. For a proof of concept, we choose a common biocompatible, low-fouling polymer, poly(ethylene glycol) (PEG), as the side chains of the pacDNA.¹⁸

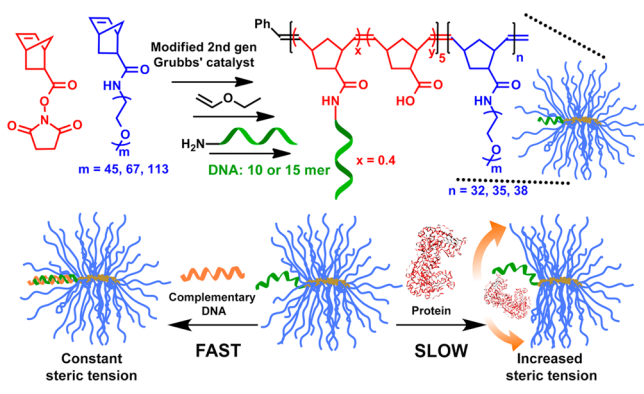
At least two parameters must be established to provide the desired binding selectivity and biological functionalities. First, the relative lengths of the PEG and the DNA must be such that the DNA can receive sufficient polymer coverage.¹⁹ Second, the PEG side chains must be dense enough to create steric congestion, requiring the brush to have sufficiently high degrees of polymerization along the backbone. Owing to recent advances of ring-opening metathesis polymerization (ROMP) and bioconjugation chemistries, control over these parameters can be easily accomplished.²⁰

To systematically probe the relationship between the structural parameters of the pacDNA and its steric selectivity, a library of six pacDNA structures have been synthesized by conjugating two DNA strands (10 or 15 bases; DNA-1:5'-NH₂-CCC AGC CCT C-F-3' and DNA-2:5'-NH₂-CCC AGC CTT CCA GCT-F-3') with three brush polymers (brushes a–c: side chain PEG M_n = 2, 3, and 5 kDa, respectively; PDI < 1.05). The brushes are

Received: July 31, 2015

Published: September 17, 2015

Scheme 1. Schematics for pacDNA Synthesis and Mechanism for Its Steric Selectivity



synthesized via sequential ROMP of norbornenyl hydroxysuccinimidyl ester (N-NHS) and norbornenyl PEG (N-PEG), to yield a diblock architecture (pN-NHS₂₋₃-b-pN-PEG₃₂₋₃₈, Table 1). The short first block containing NHS esters is incorporated for subsequent coupling with amine-modified DNA strands. Gel permeation chromatography (GPC) shows narrow molecular weight distribution for all brush polymers (Figure S1). Infrared spectroscopy shows characteristic vibrations of the NHS groups at 1739, 1780, and 1807 cm^{-1} (Figure S2), confirming their successful incorporation into the brushes.²¹ To quantify the number of reactive NHS esters available for coupling, polymers and an excess amount of fluorescein 5-thiosemicarbazide are allowed to react overnight in DMF. After removing the unreacted fluorescein by dialysis, optical absorbance was measured and compared to a standard curve to calculate the number of NHS groups per polymer (Figure S3). For brushes a–c, there are 2.1, 2.0, and 2.4 NHS esters, respectively.

For conjugation to the brushes, the DNA strands are designed to have a 5' amine group. A fluorescein tag is also incorporated at the 3' end to facilitate tracking and quantification. The conjugation is carried out in pH 8.0 bicarbonate buffer at 0 °C using an excess of DNA; the products are purified by aqueous GPC equipped with a photodiode array detector. The conjugates have a much larger molecular weight compared with that of free DNA; the two components have baseline separation (Figure S4). Agarose gel electrophoresis and GPC chromatograms for purified pacDNA show no residual free DNA (Figure S5–S6). Quantification of the number of DNA strands per brush by peak integration indicates that there are 1–2 strands for each pacDNA (Table S2), consistent with the numbers of reactive NHS ester groups. Dynamic light scattering (DLS) shows that pacDNAs have number-average hydrodynamic diameters between 25 ± 5 and 34 ± 8 nm, with narrow size distributions (PDI < 0.1, Table S2 and Figure S7). TEM shows a spherical morphology for all pacDNAs with a dry-state diameter ranging from 27 ± 4 to 31 ± 5 nm (Figure S8). The spherical morphology is not surprising because the brush polymers have relatively long side chains and short backbone length, making them structurally analogous to star polymers.²²

To examine if the brush component inhibits DNA hybridization, we adopted a fluorescence quenching assay,²³ using a quencher (dabcyl)-linked complementary DNA strand added to fluorescein-tagged pacDNA. The decrease rate of fluorescence is an indicator of the kinetics for duplex formation (Figure 1A). All pacDNAs are mixed with 2 equiv of complementary dabcyl-DNA in PBS at room temperature. A dummy strand (DNA-7) that is

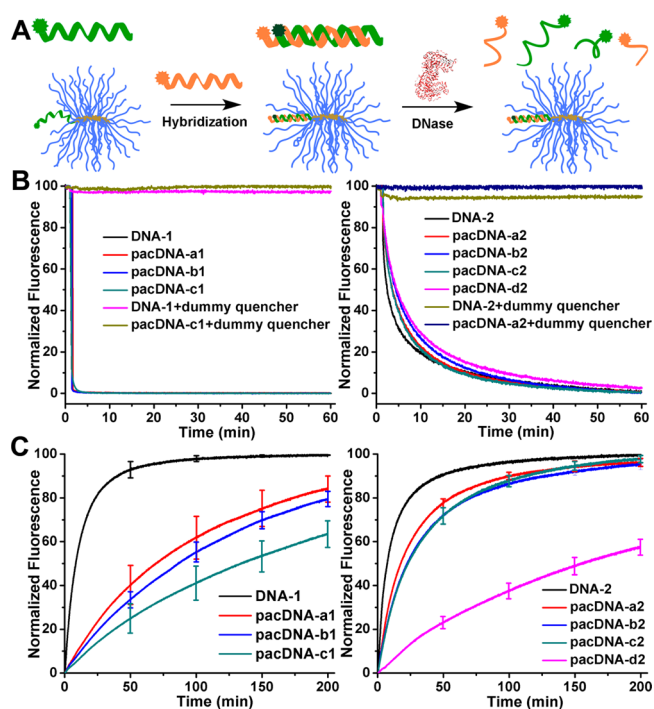


Figure 1. (A) Schematics of assays for determining DNA hybridization and nuclease degradation kinetics. (B) Hybridization kinetics for pacDNA vs free DNA. (C) Nuclease degradation kinetics for pacDNA vs free DNA.

Table 1. GPC Analyses for the Brush Polymers Used

polymer	composition	M_n (kDa)	M_w (kDa)	PDI
brush-a	pN-NHS ₂ -b-pN-PEG(2k) ₃₈	76.3	88.8	1.18
brush-b	pN-NHS ₂ -b-pN-PEG(3k) ₃₂	96.2	106.2	1.10
brush-c	pN-NHS ₂ -b-pN-PEG(5k) ₃₅	174.3	196.4	1.13
brush-d	pN-NHS ₂ -b-pN-PEG(10k) ₃₀	310.9	350.0	1.13

unable to form a duplex with the pacDNA is used as a control. Fluorescence is measured immediately upon mixing and every 3 s for 60 min. All pacDNAs hybridize immediately with their respective antisense dabcyl-DNA strands (Figure 1B), with little to no difference in the kinetics between the pacDNA and the free DNA. When the dummy dabcyl-DNA control is used in the presence of free DNA or pacDNA, fluorescence signals remain constant, ruling out nonspecific binding. There are, however, differences in the hybridization kinetics between DNA-1 and DNA-2 and between the pacDNAs containing them. This observation is likely due to the fact that DNA-2 can form a hairpin structure (calcd $T_m = 34.1$ °C). The intramolecular secondary structure stabilizes single-strand conformation and increases the energy barrier for intermolecular hybridization, slowing the hybridization kinetics.²⁴ The thermodynamics of the duplexes are not significantly changed, as manifested by the nearly identical melting transitions for pacDNA and free DNA (0.1–1.8 °C, 0.5 M NaCl, Figure S9 and Table S3).

To test if pacDNAs are able to sterically inhibit proteins from accessing their DNA component, we utilized DNase I as a model protein to act on fluorescein-pacDNAs that are prehybridized with dabcyl-DNA (Figure 1A). The fluorescence of the pacDNAs is quenched when hybridized. When DNase I is introduced, the duplexes are degraded, and the fluorophores are released, leading to an increase of fluorescence (Figure 1A). Although free DNA-1 and DNA-2 duplexes are both degraded rapidly, with half-lives of

9.3 ± 4.2 and 7.3 ± 1.7 min, respectively, all pacDNA conjugates show enhanced stability against the enzyme, as shown by prolonged half-lives and reduced initial rates (Figures 1C and S10). The best among these is pacDNA-c1, with the longest PEG side chain (5 kDa) and a shorter DNA component, showing ~14.5-fold longer half-life and ~0.09-fold the initial enzymatic activity. In contrast, pacDNA-a2, having the shortest PEG side chains (2 kDa) and the longer DNA-2, shows only ~2.4-fold increase in half-life and 0.47-fold of the initial degradation rate. We anticipate that for oligonucleotides considered for therapeutic purposes (typically 13–25 mers)²⁵ the PEG side chain M_w needs to be adjusted accordingly for optimal selectivity. Therefore, we synthesized and tested pacDNA-d2, with a longer PEG side chain (10 kDa). As predicted, pacDNA-d2 shows significantly enhanced protection for the 15-mer DNA, with 21-fold longer half-life and 0.07-fold initial degradation rate compared with those of free DNA, but its binding kinetics with complementary strands remains nearly unaffected (Figure 1). These results indicate that provided the appropriate design parameters the pacDNA can achieve substantial selectivity for DNA hybridization versus protein recognition. On the molecular level, such selectivity is possible for two reasons. First, the DNA is ~18–22 Å wide, but proteins are generally 3–10 nm in hydrodynamic diameter, giving complementary DNA a kinetic advantage for access.²⁶ Second, upon hybridization, the dsDNA does not occupy additional space relative to ssDNA; the hydrodynamic volume that it occupies does not change significantly.²⁷ In contrast, in order for a protein to access the ssDNA confined within the dense side chains, steric congestion would have to increase. Both kinetics and thermodynamics favor DNA hybridization rather than binding with a protein.

To test the inhibition of protein association in a more complex biological environment, we examined the anticoagulation properties of pacDNA versus free DNA in human plasma. Oligonucleotide sequences exhibit nonspecific and specific interactions with serum proteins, including thrombin, resulting in the prolongation of activated partial thromboplastin time (aPTT) and prothrombin time (PT).²⁸ This unwanted interaction of oligonucleotides with blood components remains a problem for intravenous gene targeting; effective control of thrombin activity and coagulation cascade is beneficial in therapeutic applications.²⁹ To test if pacDNA can restrict the access of pro/thrombin, an identified thrombin-binding aptamer (DNA-3) is used to form pacDNAs (a3, b3, and c3),^{7c} and aPTT and PT assays are carried out. Although free DNA-3 show a marked anticoagulation behavior, doubling and tripling the coagulation times in the aPTT and PT assay at 4000 nM, respectively, all pacDNAs exhibit only slight increases in clotting times in both assays compared to those of free brush-c (Figure 2). The data clearly demonstrates that pacDNA is able to inhibit the propensity of DNA to bind with serum proteins and to mask the anticoagulation effect of the DNA.

Finally, because the physical size of the brush can be tuned by controlling the degree of polymerization and side-chain length, it is possible for pacDNA to take advantage of the enhanced permeation and retention effect (EPR) for passive cancer targeting.³⁰ Being able to target cancer via EPR would necessitate sufficient blood circulation times, in turn requiring appropriate pacDNA size (10–100 nm) and low opsonization of the pacDNA surface. PacDNAs c1 and a2 are used to study in vivo biodistribution because these two structures provide a contrast in protein-shielding capabilities. To enable in vivo imaging, a near-IR tag (Cy5.5) is incorporated into the pacDNA by

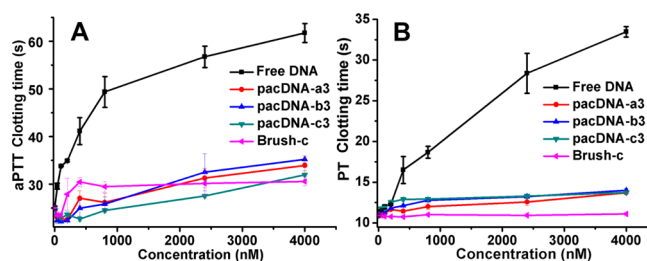


Figure 2. Blood clotting time of free DNA, brush-c, and pacDNAs vs DNA concentration in (A) aPTT and (B) PT assay.

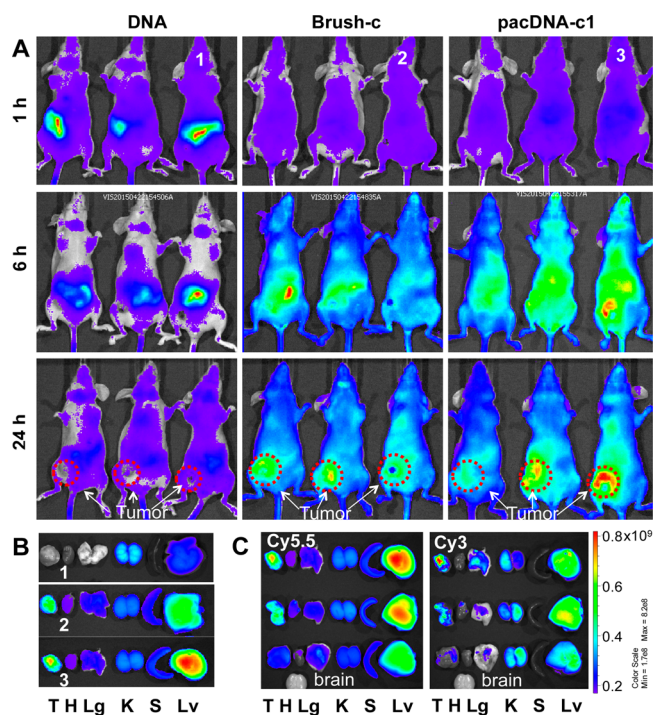


Figure 3. (A) Near-IR imaging of live mice over 24 h (Cy5.5 channel). (B) Ex vivo imaging of tissues from numbered mice (T, tumor; H, heart; Lg, lung; K, kidney; S, spleen; and Lv, liver). (C) Dual-channel imaging of organs from mice treated with dual-labeled pacDNA (polymer, Cy5.5; DNA, Cy3).

consuming a small amount of the brush NHS ester groups (<10%/mol). The DNA is modified with a Cy3 tag to allow for independent tracking. For the animal model, xenograft mice with 4T1 cells orthotopically implanted in the right mammary fat pad are used. In addition to pacDNAs, free dye, free DNA, and brush polymers are used as controls. For pacDNA-c1 and its parent polymer (brush-c), the nanostructures appear gradually on the surface of the mice after 2 h and persists for 24 h (after which mice are sacrificed), suggesting good blood circulation (Figure 3A). Significant tumor uptake is also shown in images obtained after 8 h, confirmed by ex vivo imaging of tissues at 24 h (Figure 3B). It can be seen that pacDNA-c1 shows higher liver uptake than its polymer brush counterpart, suggesting that the DNA is not completely shielded. Images of both Cy3 and Cy5.5 channels show that the signals from the DNA and the polymer components are colocalized in the tumor indicating that the DNA is successfully delivered to the tumor (Figure 3C). In contrast, lacking the shielding effect from the brush polymer, free DNA is rapidly cleared by the liver. pacDNA-a2 shows primarily hepatic uptake and minimal tumor accumulation, but its parent

polymer (brush-a) shows moderate levels of tumor uptake but is largely cleared by the kidney (Figure S12). One interpretation of these results is that pacDNA-a2 does not have sufficient shielding of the DNA and that the exposed DNA leads to the recognition and capture by liver endothelial cells.³¹ For the parent polymer brush-a, with $M_n = 76.3$ kDa, renal clearance via glomerular filtration is possible.³² These data are consistent with the fluorescence-based protein accessibility analyses (vide supra) and suggest that when designed appropriately the pacDNA can be a viable platform for systemic oligonucleotide delivery.

A novel form of brush polymer-DNA nanostructure has been developed. The densely packed side chains of the brush shield the DNA from proteins but allow unhindered DNA hybridization to take place. These structures stand apart from polycationic carrier-based approaches because the mode of NA protection is based on steric compaction instead of polyplexation, allowing noncharged polymers to be used. The pacDNA is expected to be minimally immunostimulative because the recognition of possible pathogen-associated patterns in the DNA sequence (e.g., CpG) by pattern-recognition receptors is similarly sterically hindered. We anticipate that pacDNA will exhibit significantly better biopharmaceutical characteristics compared to naked or polyplexed DNA. These data also imply that one should look beyond the chemical and biological properties of the NA and the cocarrier for oligonucleotide-based therapies to include a careful consideration of the NA's immediate local environment.

■ ASSOCIATED CONTENT

Supporting Information

The Supporting Information is available free of charge on the ACS Publications website at DOI: 10.1021/jacs.5b08069.

Materials, experimental procedures, DNA synthesis, and supplemental figures. (PDF)

■ AUTHOR INFORMATION

Corresponding Author

*k.zhang@neu.edu

Notes

The authors declare no competing financial interest.

■ ACKNOWLEDGMENTS

The authors thank William Fowle at the NEU Biology Department for help with the TEM. Financial support from Northeastern University start-up, NEU-DFCI seed grant, and NSF CAREER award (1453255) is gratefully acknowledged.

■ REFERENCES

- (1) Russell, S. J.; Peng, K.-W.; Bell, J. C. *Nat. Biotechnol.* **2012**, *30*, 658.
- (2) Freytag, S. O.; Khil, M.; Stricker, H.; Peabody, J.; Menon, M.; DePeralta-Venturina, M.; Nafziger, D.; Pegg, J.; Paielli, D.; Brown, S.; Barton, K.; Lu, M.; Aguilar-Cordova, E.; Kim, J.-H. *Cancer Res.* **2002**, *62*, 4968.
- (3) Zhang, L.; Yang, N.; Mohamed-Hadley, A.; Rubin, S. C.; Coukos, G. *Biochem. Biophys. Res. Commun.* **2003**, *303*, 1169.
- (4) Restifo, N.; Ying, H.; Hwang, L.; Leitner, W. *Gene Ther.* **2000**, *7*, 89.
- (5) (a) Rayburn, E. R.; Zhang, R. *Drug Discovery Today* **2008**, *13*, 513. (b) Hannon, G. J. *Nature* **2002**, *418*, 244. (c) Rush, A. M.; Nelles, D. A.; Blum, A. P.; Barnhill, S. A.; Tatro, E. T.; Yeo, G. W.; Gianneschi, N. C. *J. Am. Chem. Soc.* **2014**, *136*, 7615.
- (6) Abdelhady, H. G.; Allen, S.; Davies, M. C.; Roberts, C. J.; Tendler, S. J.; Williams, P. M. *Nucleic Acids Res.* **2003**, *31*, 4001.
- (7) (a) Rutz, M.; Metzger, J.; Gellert, T.; Lippa, P.; Lipford, G. B.; Wagner, H.; Bauer, S. *Eur. J. Immunol.* **2004**, *34*, 2541. (b) Medzhitov, R. *Nat. Rev. Immunol.* **2001**, *1*, 135. (c) Bock, L. C.; Griffin, L. C.; Latham, J. A.; Vermaas, E. H.; Toole, J. J. *Nature* **1992**, *355*, 564.
- (8) Hoke, G. D.; Draper, K.; Freier, S. M.; Gonzalez, C.; Driver, V. B.; Zounes, M. C.; Ecker, D. J. *Nucleic Acids Res.* **1991**, *19*, 5743.
- (9) Frieden, M.; Hansen, H. F.; Koch, T. *Nucleosides, Nucleotides Nucleic Acids* **2003**, *22*, 1041.
- (10) Meier, C.; Engels, J. W. *Angew. Chem., Int. Ed. Engl.* **1992**, *31*, 1008.
- (11) Hudziak, R. M.; Barofsky, E.; Barofsky, D. F.; Weller, D. L.; Huang, S.-B.; Weller, D. D. *Antisense Nucleic Acid Drug Dev.* **1996**, *6*, 267.
- (12) Dande, P.; Prakash, T. P.; Sioufi, N.; Gaus, H.; Jarres, R.; Berdeja, A.; Swayze, E. E.; Griffey, R. H.; Bhat, B. J. *Med. Chem.* **2006**, *49*, 1624.
- (13) (a) Lächelt, U.; Wagner, E. *Chem. Rev.* **2015**, DOI: 10.1021/cr5006793. (b) Zhang, K.; Fang, H.; Shen, G.; Taylor, J.-S. A.; Wooley, K. L. *Proc. Am. Thorac. Soc.* **2009**, *6*, 450. (c) Oh, S. S.; Lee, B. F.; Leibfarth, F. A.; Eisenstein, M.; Robb, M. J.; Lynd, N. A.; Hawker, C. J.; Soh, H. T. *J. Am. Chem. Soc.* **2014**, *136*, 15010.
- (14) Lv, H.; Zhang, S.; Wang, B.; Cui, S.; Yan, J. *J. Controlled Release* **2006**, *114*, 100.
- (15) Cutler, J. I.; Auyeung, E.; Mirkin, C. A. *J. Am. Chem. Soc.* **2012**, *134*, 1376.
- (16) Lytton-Jean, A. K.; Mirkin, C. A. *J. Am. Chem. Soc.* **2005**, *127*, 12754.
- (17) (a) Rosi, N. L.; Giljohann, D. A.; Thaxton, C. S.; Lytton-Jean, A. K.; Han, M. S.; Mirkin, C. A. *Science* **2006**, *312*, 1027. (b) Cutler, J. I.; Zhang, K.; Zheng, D.; Auyeung, E.; Prigodich, A. E.; Mirkin, C. A. *J. Am. Chem. Soc.* **2011**, *133*, 9254.
- (18) (a) Li, S.-D.; Huang, L. *J. Controlled Release* **2010**, *145*, 178. (b) van Vlerken, L. E.; Vyas, T. K.; Amiji, M. M. *Pharm. Res.* **2007**, *24*, 1405.
- (19) Zhang, K.; Zhu, X.; Jia, F.; Auyeung, E.; Mirkin, C. A. *J. Am. Chem. Soc.* **2013**, *135*, 14102.
- (20) (a) Liu, J.; Burts, A. O.; Li, Y.; Zhukhovitskiy, A. V.; Ottaviani, M. F.; Turro, N. J.; Johnson, J. A. *J. Am. Chem. Soc.* **2012**, *134*, 16337. (b) Zhang, Y.; Yin, Q.; Lu, H.; Xia, H.; Lin, Y.; Cheng, J. *ACS Macro Lett.* **2013**, *2*, 809. (c) Gutekunst, W. R.; Hawker, C. J. *J. Am. Chem. Soc.* **2015**, *137*, 8038. (d) Jia, F.; Lu, X.; Tan, X.; Zhang, K. *Chem. Commun.* **2015**, *51*, 7843.
- (21) Lu, X.; Watts, E.; Jia, F.; Tan, X.; Zhang, K. *J. Am. Chem. Soc.* **2014**, *136*, 10214.
- (22) (a) Pesek, S. L.; Li, X.; Hammouda, B.; Hong, K.; Verduzco, R. *Macromolecules* **2013**, *46*, 6998. (b) Gao, H. *Macromol. Rapid Commun.* **2012**, *33*, 722.
- (23) (a) Seferos, D. S.; Prigodich, A. E.; Giljohann, D. A.; Patel, P. C.; Mirkin, C. A. *Nano Lett.* **2009**, *9*, 308. (b) Tan, X.; Li, B. B.; Lu, X.; Jia, F.; Santori, C.; Menon, P.; Li, H.; Zhang, B.; Zhao, J. J.; Zhang, K. *J. Am. Chem. Soc.* **2015**, *137*, 6112.
- (24) Chen, C.; Wang, W.; Wang, Z.; Wei, F.; Zhao, X. S. *Nucleic Acids Res.* **2007**, *35*, 2875.
- (25) (a) Dias, N.; Stein, C. *Mol. Cancer Therapeut.* **2002**, *1*, 347. (b) Roh, H.; Pippin, J.; Drebin, J. A. *Cancer Res.* **2000**, *60*, 560.
- (26) Erickson, H. P. *Biol. Proced. Online* **2009**, *11*, 32.
- (27) (a) Seeman, N. C. *Nature* **2003**, *421*, 427. (b) Mills, J. B.; Vacano, E.; Hagerman, P. J. *J. Mol. Biol.* **1999**, *285*, 245.
- (28) (a) Lebedeva, I.; Stein, C. *Annu. Rev. Pharmacol. Toxicol.* **2001**, *41*, 403. (b) Henry, S. P.; Novotny, W.; Leeds, J.; Auletta, C.; Kornbrust, D. *J. Antisense Nucleic Acid Drug Dev.* **1997**, *7*, 503.
- (29) (a) Chan, J. H.; Lim, S.; Wong, W. *Clin. Exp. Pharmacol. Physiol.* **2006**, *33*, 533. (b) Ogris, M.; Brunner, S.; Schüller, S.; Kircheis, R.; Wagner, E. *Gene Ther.* **1999**, *6*, 595.
- (30) (a) Wang, J.; Mao, W.; Lock, L. L.; Tang, J.; Sui, M.; Sun, W.; Cui, H.; Xu, D.; Shen, Y. *ACS Nano* **2015**, *9*, 7195. (b) Maeda, H.; Wu, J.; Sawa, T.; Matsumura, Y.; Hori, K. *J. Controlled Release* **2000**, *65*, 271.
- (31) Seternes, T.; Sørensen, K.; Smedsrød, B. *Proc. Natl. Acad. Sci. U. S. A.* **2002**, *99*, 7594.
- (32) Ruggiero, A.; Villa, C. H.; Bander, E.; Rey, D. A.; Bergkvist, M.; Batt, C. A.; Manova-Todorova, K.; Deen, W. M.; Scheinberg, D. A.; McDevitt, M. R. *Proc. Natl. Acad. Sci. U. S. A.* **2010**, *107*, 12369.